Chapter 5
Topology Design Optimization

In this chapter a topology optimization algorithm based on the topological derivative concept combined with a level-set domain representation method is presented [11], together with its applications in the context of compliance structural topology optimization and topology design of compliant mechanisms. It is worth mentioning that the topological derivative is defined through a limit passage when the small parameter governing the size of the topological perturbation goes to zero. Therefore, it can be used as a steepest-descent direction in an optimization process, according to any method based on the gradient of the cost functional. We restrict ourselves to the case in which the domain is topologically perturbed by the nucleation of a small inclusion where a weak material phase is used to mimic voids, allowing to work in a fixed computational domain. This simple strategy bypasses the use of a complicated algorithm specifically designed to deal with nucleation of holes in a computational domain.

Let us introduce a hold-all domain $\mathscr{D} \subset \mathbb{R}^2$, which is split into two subdomains, $\Omega \subset \mathscr{D}$ and its complement $\mathscr{D} \setminus \Omega$. We assume that there is a distributed parameter $\rho : \mathscr{D} \mapsto \{1, \rho_0\}$ defined as

$$\rho(x) := \begin{cases} 1 & \text{if } x \in \Omega, \\ \rho_0 & \text{if } x \in \mathscr{D} \setminus \Omega, \end{cases} \tag{5.1}$$

with $0 < \rho_0 \ll 1$. The topology optimization problem we are dealing with consists in minimizing a shape functional $\Omega \mapsto J(\Omega)$ with respect to $\Omega \subset \mathscr{D}$, that is:

$$\underset{\Omega \subset \mathscr{D}}{\text{Minimize}}\ J(\Omega)\ , \tag{5.2}$$

which can be solved by using the topological derivative concept. Actually, a circular hole $B_\varepsilon(\widehat{x})$ is introduced inside $\mathscr{D}$. Then, the region occupied by $B_\varepsilon(\widehat{x})$ is filled by

A. A. Novotny, J. Sokołowski, *An Introduction to the Topological Derivative Method*, SpringerBriefs in Mathematics,
https://doi.org/10.1007/978-3-030-36915-6_5

an inclusion with material properties different from the background. The material properties are characterized by a piecewise constant function γ_ε of the form

$$\gamma_\varepsilon(x) := \begin{cases} 1 & \text{if } x \in \mathscr{D} \setminus \overline{B_\varepsilon}\,, \\ \gamma(x) & \text{if } x \in B_\varepsilon\,, \end{cases} \tag{5.3}$$

where the *contrast* γ is defined as

$$\gamma(x) = \begin{cases} \rho_0 & \text{if } x \in \Omega, \\ \rho_0^{-1} & \text{if } x \in \mathscr{D} \setminus \Omega, \end{cases} \tag{5.4}$$

which induces a level-set domain representation method.

In order to fix these ideas, a model problem in elasticity is considered in Sect. 5.1. The resulting topology design algorithm based on the topological derivative concept combined with a level-set domain representation method is presented in Sect. 5.2. Some numerical results in the context of compliance structural topology optimization and topology design of compliant mechanisms are presented in Sect. 5.3. Finally, the chapter ends in Sect. 5.4 with a discussion concerning perspectives of future developments, together with a list of open problems.

5.1 Model Problem in Elasticity

In this section, the topological derivative of a tracking-type shape functional associated with the linear elasticity problem into two spatial dimensions, in the presence of an small circular inclusion, is derived.

The tracking-type shape functional associated with the unperturbed domain is defined as

$$\psi(\chi) := \mathscr{J}(u) = \int_{\Gamma_N} g \cdot u\,, \tag{5.5}$$

where g is a given vector function in $H^{-1/2}(\Gamma_N)$ and the displacement vector field $u : \mathscr{D} \mapsto \mathbb{R}^2$ is the solution of the following variational problem:

$$u \in \mathscr{U} : \int_{\mathscr{D}} \sigma(u) \cdot (\nabla \eta)^s = \int_{\Gamma_N} q \cdot \eta \quad \forall \eta \in \mathscr{V}\,, \tag{5.6}$$

with $\sigma(u) = \rho \mathbb{C} (\nabla u)^s$. In the above equation, ρ is given by (5.1), $q \in H^{-1/2}(\Gamma_N)$ is a given boundary traction, and $(\nabla \varphi)^s$ is the symmetric part of the gradient of a vector field φ, namely

$$(\nabla \varphi)^s := \frac{1}{2} \left(\nabla \varphi + (\nabla \varphi)^\top \right)\,. \tag{5.7}$$

By considering isotropic medium, the constitutive tensor $\mathbb{C}$ can be represented as

$$\mathbb{C} = 2\mu\,\mathbb{I} + \lambda\,\mathrm{I}\otimes\mathrm{I}\,, \tag{5.8}$$

where I and $\mathbb{I}$ are identity tensors of second and fourth orders, respectively, and μ and λ are the Lamé coefficients, both considered constants everywhere. In particular, in the case of plane stress assumptions, we have

$$\mu = \frac{E}{2(1+\nu)} \quad \text{and} \quad \lambda = \frac{\nu E}{1-\nu^2}\,, \tag{5.9}$$

whereas in the case of plane strain state, there are

$$\mu = \frac{E}{2(1+\nu)} \quad \text{and} \quad \lambda = \frac{\nu E}{(1+\nu)(1-2\nu)}\,, \tag{5.10}$$

where E is the Young modulus and ν the Poisson ratio. The spaces $\mathscr{U}$ and $\mathscr{V}$ are defined as

$$\mathscr{U} = \mathscr{V} = \left\{\varphi \in H^1(\mathscr{D}) : \varphi_{|\Gamma_D} = 0\right\}. \tag{5.11}$$

In addition, $\partial\mathscr{D} = \Gamma_D \cup \Gamma_N$ with $\Gamma_D \cap \Gamma_N = \varnothing$, where Γ_D and Γ_N are Dirichlet and Neumann boundaries, respectively. See sketch in Fig. 5.1.

The strong system associated with the variational problem (5.6) can be stated as: Find u, such that

$$\begin{cases} \operatorname{div}\sigma(u) = 0 & \text{in } \mathscr{D}\,, \\ \sigma(u) = \rho\mathbb{C}(\nabla u)^s & \\ u = 0 & \text{on } \Gamma_D\,, \\ \sigma(u)n = q & \text{on } \Gamma_N\,. \end{cases} \tag{5.12}$$

Remark 5.1 By setting $\rho(x) = 1\ \forall x \in \mathscr{D}$ in (5.1), the boundary value problem (5.12) degenerates itself to the well-known Navier system, namely

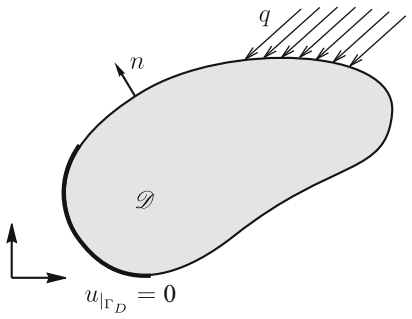

Fig. 5.1 The elasticity problem defined in the unperturbed domain

$$\mu \Delta u + (\lambda + \mu) \nabla (\operatorname{div} u) = 0 \quad \text{in} \quad \mathscr{D} \,, \tag{5.13}$$

where μ and λ are the Lamé coefficients given by (5.9) for the plane stress case and by (5.10) for the plane strain assumption.

In order to simplify further analysis, an auxiliary vector function $v : \mathscr{D} \mapsto \mathbb{R}^2$ is introduced, which is the solution of the following *adjoint variation problem* (see Sect. 1.2.1 for details)

$$v \in \mathscr{V} : \int_{\mathscr{D}} \sigma(v) \cdot (\nabla \eta)^s = - \int_{\Gamma_N} g \cdot \eta \quad \forall \eta \in \mathscr{V} \,, \tag{5.14}$$

with $\sigma(v) = \rho \mathbb{C} (\nabla v)^s$.

Remark 5.2 (Lagrangian Formalism) As discussed in Sect. 1.2.1, the adjoint state v solution of (5.14) comes out from the Lagrangian formalism. In particular, the basic idea consists in defining a Lagrangian functional given by the sum of the shape functional (5.5) and the state equation in its weak form (5.6), namely

$$\mathscr{L}(u, v) := \int_{\Gamma_N} g \cdot u + \int_{\mathscr{D}} \sigma(u) \cdot (\nabla v)^s - \int_{\Gamma_N} q \cdot v \,. \tag{5.15}$$

By applying the first order optimality condition in (5.15) with respect to $v \in \mathscr{V}$, we recover the state equation (5.6), that is

$$u \in \mathscr{U} \;\; : \int_{\mathscr{D}} \sigma(u) \cdot (\nabla \eta)^s - \int_{\Gamma_N} q \cdot \eta = 0 \quad \forall \eta \in \mathscr{V} \,. \tag{5.16}$$

On the other hand, after applying the first order optimality condition in (5.15) with respect to $u \in \mathscr{U}$, we obtain

$$v \in \mathscr{V} \;\; : \int_{\mathscr{D}} \sigma(\eta) \cdot (\nabla v)^s + \int_{\Gamma_N} g \cdot \eta = 0 \quad \forall \eta \in \mathscr{V} \,, \tag{5.17}$$

which is actually the adjoint equation (5.14), since the bilinear form on the left-hand side of (5.17) is symmetric. It is also important to note that the adjoint state v always belongs to the space $\mathscr{V}$. Therefore, in our particular case, we have just used the symmetry of the bilinear form to define the adjoint problem according to (5.14) and the fact that $\mathscr{U} = \mathscr{V}$.

Remark 5.3 (Self Adjoint Problem) Note also that by setting $g = q$ in (5.5), the tracking-type shape functional becomes the structural compliance, which has been taken into account in Chap. 3. In this particular case, the problem is self-adjoint in the sense that after replacing g by q in the right-hand side of the adjoint equation (5.14), we can compare with the state equation (5.6) and conclude that $v = -u$ for $g = q$, provided that $\mathscr{U} = \mathscr{V}$ according to (5.11).

Now, let us state the perturbed counterpart of the problem. In particular, the tracking-type shape functional associated with the topologically perturbed domain can be written as

$$\psi(\chi_\varepsilon) := \mathscr{J}_\varepsilon(u_\varepsilon) = \int_{\Gamma_N} g \cdot u_\varepsilon \ . \tag{5.18}$$

The displacement vector field $u_\varepsilon : \mathscr{D} \mapsto \mathbb{R}^2$ solves the following variational problem:

$$u_\varepsilon \in \mathscr{U} : \int_{\mathscr{D}} \sigma_\varepsilon(u_\varepsilon) \cdot (\nabla \eta)^s = \int_{\Gamma_N} q \cdot \eta \quad \forall \eta \in \mathscr{V} \ , \tag{5.19}$$

with $\sigma_\varepsilon(u_\varepsilon) = \gamma_\varepsilon \rho \mathbb{C}(\nabla u_\varepsilon)^s$, where the contrast γ_ε is given by (5.3). The *strong system* associated with the variational problem (5.19) can be written as: Find u_ε, such that

$$\left\{ \begin{array}{rcll} \operatorname{div} \sigma_\varepsilon(u_\varepsilon) & = & 0 & \text{in } \mathscr{D} \ , \\ \sigma_\varepsilon(u_\varepsilon) & = & \gamma_\varepsilon \rho \mathbb{C}(\nabla u_\varepsilon)^s & \\ u_\varepsilon & = & 0 & \text{on } \Gamma_D \ , \\ \sigma(u_\varepsilon) n & = & q & \text{on } \Gamma_N \ , \\ \left. \begin{array}{r} [\![u_\varepsilon]\!] = 0 \\ [\![\sigma_\varepsilon(u_\varepsilon)]\!] n = 0 \end{array} \right\} & & & \text{on } \partial B_\varepsilon \ , \end{array} \right. \tag{5.20}$$

where the operator $[\![\varphi]\!]$ is used to denote the jump of function φ on the boundary of the inclusion ∂B_ε, namely $[\![\varphi]\!] := \varphi_{|_{\mathscr{D} \setminus \overline{B_\varepsilon}}} - \varphi_{|_{B_\varepsilon}}$ on ∂B_ε. See details in Fig. 5.2. Note that the *transmission condition* on the interface ∂B_ε comes out from the variational formulation (5.19).

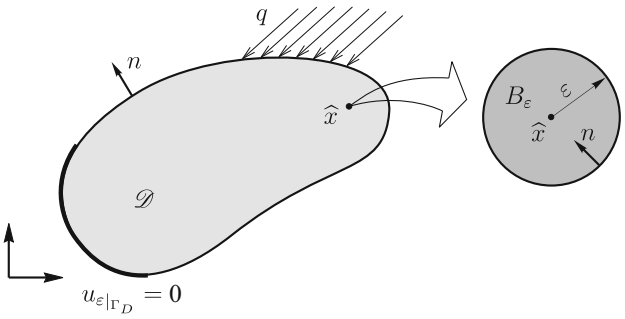

Fig. 5.2 The elasticity problem defined in the perturbed domain

5.1.1 Existence of the Topological Derivative

The following lemma ensures the existence of the associated topological derivative:

Lemma 5.1 *Let u and u_ε be the solutions of the original (5.6) and perturbed (5.19) problems, respectively. Then, the following estimate holds true:*

$$\|u_\varepsilon - u\|_{H^1(\mathscr{D})} \leq C\varepsilon \,, \tag{5.21}$$

where C is a constant independent of the control parameter ε.

Proof From the definition of the contrast γ_ε given by (5.3), we have that Eq. (5.6) can be rewritten as

$$\int_{\mathscr{D}\setminus\overline{B_\varepsilon}} \sigma(u)\cdot(\nabla\eta)^s + \int_{B_\varepsilon} \sigma(u)\cdot(\nabla\eta)^s \pm \int_{B_\varepsilon} \gamma\sigma(u)\cdot(\nabla\eta)^s = \int_{\Gamma_N} q\cdot\eta \,, \tag{5.22}$$

or even as

$$u \in \mathscr{U} \;:\; \int_{\mathscr{D}} \sigma_\varepsilon(u)\cdot(\nabla\eta)^s + (1-\gamma)\int_{B_\varepsilon} \sigma(u)\cdot(\nabla\eta)^s = \int_{\Gamma_N} \overline{q}\cdot\eta \quad \forall\eta \in \mathscr{V} \,. \tag{5.23}$$

By taking $\eta = u_\varepsilon - u$ as test function in the above equation and also in (5.19), there are

$$\int_{\mathscr{D}} \sigma_\varepsilon(u)\cdot\nabla(u_\varepsilon - u)^s = \int_{\Gamma_N} q\cdot(u_\varepsilon - u) - (1-\gamma)\int_{B_\varepsilon} \sigma(u)\cdot\nabla(u_\varepsilon - u)^s \,, \tag{5.24}$$

$$\int_{\mathscr{D}} \sigma_\varepsilon(u_\varepsilon)\cdot\nabla(u_\varepsilon - u)^s = \int_{\Gamma_N} q\cdot(u_\varepsilon - u) \,. \tag{5.25}$$

After subtracting the first equation from the second one, we obtain the following equality:

$$\int_{\mathscr{D}} \sigma_\varepsilon(u_\varepsilon - u)\cdot\nabla(u_\varepsilon - u)^s = (1-\gamma)\int_{B_\varepsilon} \sigma(u)\cdot\nabla(u_\varepsilon - u)^s \,. \tag{5.26}$$

The Cauchy–Schwarz inequality implies

$$\begin{aligned}\int_{\mathscr{D}} \sigma_\varepsilon(u_\varepsilon - u)\cdot\nabla(u_\varepsilon - u)^s &\leq C_1\|\sigma(u)\|_{L^2(B_\varepsilon)}\|\nabla(u_\varepsilon - u)^s\|_{L^2(B_\varepsilon)} \\ &\leq C_2\varepsilon\|u_\varepsilon - u\|_{H^1(\mathscr{D})} \,,\end{aligned} \tag{5.27}$$

where we have used the interior elliptic regularity of u. Finally, from the *coercivity* of the bilinear form on the left-hand side of the above inequality, namely

$$c\|u_\varepsilon - u\|^2_{H^1(\mathscr{D})} \leq \int_{\mathscr{D}} \sigma_\varepsilon(u_\varepsilon - u) \cdot \nabla(u_\varepsilon - u)^s \ , \tag{5.28}$$

we obtain

$$\|u_\varepsilon - u\|^2_{H^1(\mathscr{D})} \leq C\varepsilon \|u_\varepsilon - u\|_{H^1(\mathscr{D})} \ , \tag{5.29}$$

which leads to the result with $C = C_2/c$. □

5.1.2 Variation of the Shape Functional

From a simple manipulation and with the help of the adjoint equation (5.14), it is possible to write the variation of the shape functional in terms of an integral concentrated in the ball B_ε. In fact, after subtracting (5.5) from (5.18) we obtain

$$\mathscr{J}_\varepsilon(u_\varepsilon) - \mathscr{J}(u) = \int_{\Gamma_N} g \cdot (u_\varepsilon - u) \ . \tag{5.30}$$

From the definition for the contrast γ_ε given by (5.3), the state equation associated with the topologically perturbed domain (5.19) can be rewritten as

$$\int_{\mathscr{D}\setminus\overline{B_\varepsilon}} \sigma(u_\varepsilon) \cdot (\nabla\eta)^s + \int_{B_\varepsilon} \gamma\sigma(u_\varepsilon) \cdot (\nabla\eta)^s \pm \int_{B_\varepsilon} \sigma(u_\varepsilon) \cdot (\nabla\eta)^s = \int_{\Gamma_N} q \cdot \eta \ . \tag{5.31}$$

Therefore, it follows that

$$\int_{\mathscr{D}} \sigma(u_\varepsilon) \cdot (\nabla\eta)^s = (1-\gamma) \int_{B_\varepsilon} \sigma(u_\varepsilon) \cdot (\nabla\eta)^s + \int_{\Gamma_N} q \cdot \eta \ . \tag{5.32}$$

Now, we can subtract the state equation associated with the unperturbed domain (5.6) from the above result to obtain

$$\int_{\mathscr{D}} \sigma(u_\varepsilon - u) \cdot (\nabla\eta)^s = (1-\gamma) \int_{B_\varepsilon} \sigma(u_\varepsilon) \cdot (\nabla\eta)^s \ . \tag{5.33}$$

By choosing $\eta = v$ as test function in the above equation, where v is the adjoint state solution of (5.14), we have

$$\int_{\mathscr{D}} \sigma(u_\varepsilon - u) \cdot (\nabla v)^s = (1-\gamma) \int_{B_\varepsilon} \sigma(u_\varepsilon) \cdot (\nabla v)^s \ . \tag{5.34}$$

On the other hand, by setting $\eta = u_\varepsilon - u$ as test function in the adjoint equation (5.14), there is

$$\int_{\mathscr{D}} \sigma(v) \cdot (\nabla(u_\varepsilon - u))^s = -\int_{\Gamma_N} g \cdot (u_\varepsilon - u) \, . \tag{5.35}$$

Since the bilinear forms on the left-hand side of the above two last equations are symmetric, then we obtain the following important equality:

$$\int_{\Gamma_N} g \cdot (u_\varepsilon - u) = -(1-\gamma) \int_{B_\varepsilon} \sigma(u_\varepsilon) \cdot (\nabla v)^s \, . \tag{5.36}$$

After comparing the above result with (5.30), we conclude that

$$\mathscr{J}_\varepsilon(u_\varepsilon) - \mathscr{J}(u) = -(1-\gamma) \int_{B_\varepsilon} \sigma(u_\varepsilon) \cdot (\nabla v)^s \, . \tag{5.37}$$

Therefore, thanks to the adjoint state v solution of (5.14), the variation of the shape functional can, in fact, be written in terms of an integral concentrated in the ball B_ε. Before proceeding, let us sum and subtract the term

$$-(1-\gamma) \int_{B_\varepsilon} \sigma(u) \cdot (\nabla v)^s \tag{5.38}$$

from (5.37) to obtain

$$\mathscr{J}_\varepsilon(u_\varepsilon) - \mathscr{J}(u) = -(1-\gamma) \int_{B_\varepsilon} \sigma(u) \cdot (\nabla v)^s + \mathscr{I}(\varepsilon) \, . \tag{5.39}$$

The integral $\mathscr{I}(\varepsilon)$ is defined as

$$\mathscr{I}(\varepsilon) = -(1-\gamma) \int_{B_\varepsilon} \sigma(u_\varepsilon - u) \cdot (\nabla v)^s \, , \tag{5.40}$$

which can be bounded as follows:

$$\begin{aligned} |\mathscr{I}(\varepsilon)| &\leq C_1 \|\nabla v\|_{L^2(B_\varepsilon)} \|\sigma(u_\varepsilon - u)\|_{L^2(B_\varepsilon)} \\ &\leq C_2 \varepsilon \|u_\varepsilon - u\|_{H^1(\Omega)} \leq C_3 \varepsilon^2 = O(\varepsilon^2) \, , \end{aligned} \tag{5.41}$$

where we have used Lemma 5.1, together with the interior elliptic regularity of function u. According to Lemma 5.1, a leading term of order $O(\varepsilon^2)$ is expected. On the other hand, the above estimate cannot be improved, so that there is a nontrivial term of order $O(\varepsilon^2)$ hidden in (5.40). In the next section we will show how to extract such a leading term of order $O(\varepsilon^2)$ from (5.40).

5.1.3 Asymptotic Analysis of the Solution

The variation of the tracking-type shape functional has been written exclusively in terms of an integral concentrated in the ball B_ε, as shown through (5.37). In order to obtain the associated topological asymptotic expansion in the form of (1.2), we need to know the asymptotic behavior of the solution u_ε with respect to ε in the neighborhood of the ball B_ε. In particular, once knowing explicitly such a behavior, function $f(\varepsilon)$ can be identified, which allows for evaluating the limit $\varepsilon \to 0$ in (1.4), leading to the final formula for the topological derivative $\mathscr{T}$ of the shape functional ψ. Therefore, the basic idea consists in expanding u_ε asymptotically with respect to the small parameter ε. In this section, we obtain the asymptotic expansion of the solution u_ε associated with the transmission condition on the boundary ∂B_ε of the inclusion. We start by proposing an *ansatz* for u_ε in the form [58]

$$u_\varepsilon(x) = u(x) + w_\varepsilon(x) + \widetilde{u}_\varepsilon(x) \; . \tag{5.42}$$

After applying the operator $\sigma_\varepsilon = \gamma_\varepsilon \sigma$, we have

$$\begin{aligned} \sigma_\varepsilon(u_\varepsilon(x)) &= \sigma_\varepsilon(u(x)) + \sigma_\varepsilon(w_\varepsilon(x)) + \sigma_\varepsilon(\widetilde{u}_\varepsilon(x)) \\ &= \gamma_\varepsilon \sigma(u(\widehat{x})) + \gamma_\varepsilon(\sigma(u(x)) - \sigma(u(\widehat{x})) + \sigma_\varepsilon(w_\varepsilon(x)) + \sigma_\varepsilon(\widetilde{u}_\varepsilon(x)) \end{aligned} \tag{5.43}$$

On the boundary of the inclusion ∂B_ε there is

$$[\![\sigma_\varepsilon(u_\varepsilon)]\!] n = 0 \quad \Rightarrow \quad (\sigma(u_\varepsilon)_{|_{\mathscr{D}\setminus\overline{B_\varepsilon}}} - \gamma\sigma(u_\varepsilon)_{|_{B_\varepsilon}})n = 0 \; , \tag{5.44}$$

so that the above expansion evaluated on ∂B_ε yields

$$\begin{aligned} &(1-\gamma)\sigma(u(\widehat{x}))n + (1-\gamma)(\sigma(u(x)) - \sigma(u(\widehat{x}))n \\ &\quad + [\![\sigma_\varepsilon(w_\varepsilon(x))]\!] n + [\![\sigma_\varepsilon(\widetilde{u}_\varepsilon(x))]\!] n = 0 \; , \end{aligned} \tag{5.45}$$

which allows for choosing the jump $[\![\sigma_\varepsilon(w_\varepsilon(x))]\!] n$ on ∂B_ε as

$$[\![\sigma_\varepsilon(w_\varepsilon(x))]\!] n = -(1-\gamma)\sigma(u(\widehat{x}))n \quad \text{on} \quad \partial B_\varepsilon \; . \tag{5.46}$$

Now, the following *exterior problem* is formally defined with $\varepsilon \to 0$: Find $\sigma_\varepsilon(w_\varepsilon)$, such that

$$\left\{ \begin{array}{l} \operatorname{div} \sigma_\varepsilon(w_\varepsilon) = 0 \text{ in } \mathbb{R}^2 \; , \\ \quad \sigma_\varepsilon(w_\varepsilon) \to 0 \text{ at } \infty \; , \\ [\![\sigma_\varepsilon(w_\varepsilon)]\!] n = \widehat{v} \text{ on } \partial B_\varepsilon \; , \end{array} \right. \tag{5.47}$$

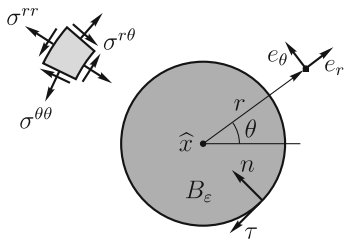

Fig. 5.3 Polar coordinate system (r, θ) centered at the point $\widehat{x}$

where $\widehat{v} = -(1-\gamma)\sigma(u(\widehat{x}))n$. The above boundary value problem admits an *explicit solution* (see, for instance, the book by Little [62]), which can be written in a polar coordinate system (r, θ) with center at $\widehat{x}$ (see Fig. 5.3) as follows:

- For $r \geq \varepsilon$ (outside the inclusion)

$$\sigma_\varepsilon^{rr}(w_\varepsilon(r,\theta)) = -\varphi_1 \left(\tfrac{1-\gamma}{1+\gamma a_1}\tfrac{\varepsilon^2}{r^2}\right) - \varphi_2 \left(4\tfrac{1-\gamma}{1+\gamma a_2}\tfrac{\varepsilon^2}{r^2} + 3\tfrac{1-\gamma}{1+\gamma a_2}\tfrac{\varepsilon^4}{r^4}\right)\cos 2\theta \ , \tag{5.48}$$

$$\sigma_\varepsilon^{\theta\theta}(w_\varepsilon(r,\theta)) = \varphi_1 \left(\tfrac{1-\gamma}{1+\gamma a_1}\tfrac{\varepsilon^2}{r^2}\right) - \varphi_2 \left(3\tfrac{1-\gamma}{1+\gamma a_2}\tfrac{\varepsilon^4}{r^4}\right)\cos 2\theta \ , \tag{5.49}$$

$$\sigma_\varepsilon^{r\theta}(w_\varepsilon(r,\theta)) = -\varphi_2 \left(2\tfrac{1-\gamma}{1+\gamma a_2}\tfrac{\varepsilon^2}{r^2} - 3\tfrac{1-\gamma}{1+\gamma a_2}\tfrac{\varepsilon^4}{r^4}\right)\sin 2\theta \ . \tag{5.50}$$

- For $0 < r < \varepsilon$ (inside the inclusion)

$$\sigma_\varepsilon^{rr}(w_\varepsilon(r,\theta)) = \varphi_1 \left(a_1\gamma\tfrac{1-\gamma}{1+\gamma a_1}\right) + \varphi_2 \left(a_2\gamma\tfrac{1-\gamma}{1+\gamma a_2}\right)\cos 2\theta \ , \tag{5.51}$$

$$\sigma_\varepsilon^{\theta\theta}(w_\varepsilon(r,\theta)) = \varphi_1 \left(a_1\gamma\tfrac{1-\gamma}{1+\gamma a_1}\right) - \varphi_2 \left(a_2\gamma\tfrac{1-\gamma}{1+\gamma a_2}\right)\cos 2\theta \ , \tag{5.52}$$

$$\sigma_\varepsilon^{r\theta}(w_\varepsilon(r,\theta)) = -\varphi_2 \left(a_2\gamma\tfrac{1-\gamma}{1+\gamma a_2}\right)\sin 2\theta \ . \tag{5.53}$$

Some terms in the above formulae require explanations. The coefficients φ_1 and φ_2 are given by

$$\varphi_1 = \frac{1}{2}(\sigma_1(u(\widehat{x})) + \sigma_2(u(\widehat{x}))) \ , \quad \varphi_2 = \frac{1}{2}(\sigma_1(u(\widehat{x})) - \sigma_2(u(\widehat{x}))) \ , \tag{5.54}$$

where $\sigma_1(u(\widehat{x}))$ and $\sigma_2(u(\widehat{x}))$ are the eigenvalues of tensor $\sigma(u(\widehat{x}))$, which can be expressed as (see Appendix A, identity (A.52))

$$\sigma_{1,2}(u(\widehat{x})) = \frac{1}{2}\left(\operatorname{tr}\sigma(u(\widehat{x})) \pm \sqrt{2\sigma^D(u(\widehat{x}))\cdot\sigma^D(u(\widehat{x}))}\right) \ , \tag{5.55}$$

with $\sigma^D(u(\widehat{x}))$ standing for the deviatory part of the stress tensor $\sigma(u(\widehat{x}))$, namely

$$\sigma^D(u(\widehat{x})) = \sigma(u(\widehat{x})) - \frac{1}{2}\mathrm{tr}\,\sigma(u(\widehat{x}))\mathrm{I}\,. \tag{5.56}$$

In addition, the constants a_1 and a_2 are given by

$$a_1 = \frac{\mu+\lambda}{\mu} \quad \text{e} \quad a_2 = \frac{3\mu+\lambda}{\mu+\lambda}\,. \tag{5.57}$$

Finally, $\sigma_\varepsilon^{rr}(u_\varepsilon)$, $\sigma_\varepsilon^{\theta\theta}(u_\varepsilon)$, and $\sigma_\varepsilon^{r\theta}(u_\varepsilon)$ are the components of tensor $\sigma_\varepsilon(u_\varepsilon)$ in the polar coordinate system, namely $\sigma_\varepsilon^{rr}(u_\varepsilon) = e^r \cdot \sigma_\varepsilon(u_\varepsilon)e^r$, $\sigma_\varepsilon^{\theta\theta}(u_\varepsilon) = e^\theta \cdot \sigma_\varepsilon(u_\varepsilon)e^\theta$, and $\sigma_\varepsilon^{r\theta}(u_\varepsilon) = \sigma_\varepsilon^{\theta r}(u_\varepsilon) = e^r \cdot \sigma_\varepsilon(u_\varepsilon)e^\theta$, with e^r and e^θ used to denote the canonical basis associated with the polar coordinate system (r,θ), such that, $\|e^r\| = \|e^\theta\| = 1$ and $e^r \cdot e^\theta = 0$. See Appendix A.

Remark 5.4 (Eshelby's Theorem) According to (5.51)–(5.53), we observe that the stress tensor field associated with the solution of the exterior problem (5.47) is uniform inside the inclusion $B_\varepsilon(\widehat{x})$. It means that the stress acting in the inclusion embedded in the whole two-dimensional space $\mathbb{R}^2$ can be written in the following compact form:

$$\sigma_\varepsilon(w_\varepsilon(x))_{|_{B_\varepsilon(\widehat{x})}} = \gamma\,\mathbb{T}\sigma(u(\widehat{x}))\,, \tag{5.58}$$

where $\mathbb{T}$ is a fourth order uniform (constant) tensor given by

$$\mathbb{T} = \frac{1}{2}\frac{1-\gamma}{1+\gamma a_2}\left(2a_2\mathbb{I} + \frac{a_1-a_2}{1+\gamma a_1}\mathrm{I}\otimes\mathrm{I}\right)\,. \tag{5.59}$$

Therefore, the above result fits the famous Eshelby's problem. This problem, formulated by Eshelby in 1957 [38] and 1959 [39], represents one of the major advances in the continuum mechanics theory of the twentieth century [56]. It plays a central role in the theory of elasticity involving the determination of effective elastic properties of materials with multiple inhomogeneities. For more details, see the book by Mura [70], for instance. The Eshelby's problem, also referred to as the Eshelby's theorem, is also related to the Polarization tensor in asymptotic analysis of the strain energy with respect to singular domain perturbations [71]. In fact, tensor $\mathbb{T}$ represents one term contribution to the Polarization tensor coming from the solution to the exterior problem (5.47). In the next section we will apply the Eshelby's theorem to the derivation of the polarization tensor and to the topological derivative evaluation as well. Concerning applications of the Eshelby's theorem to the problem of optimal patch in elasticity, see [61, 72].

Now, we can construct the remainder $\widetilde{u}_\varepsilon$ from (5.42) in such a way that it compensates for the discrepancies produced by the higher order terms in ε as well as by the boundary layer w_ε on the exterior boundary $\partial\mathscr{D}$. It means that the *remainder* $\widetilde{u}_\varepsilon$ has to be the solution of the following boundary value problem: Find $\widetilde{u}_\varepsilon$, such that

$$\left\{\begin{array}{rcll} \operatorname{div}\sigma_\varepsilon(\widetilde{u}_\varepsilon) &=& 0 & \text{in } \mathscr{D}\ , \\ \sigma_\varepsilon(\widetilde{u}_\varepsilon) &=& \gamma_\varepsilon\rho\mathbb{C}(\nabla\widetilde{u}_\varepsilon)^s & \\ \widetilde{u}_\varepsilon &=& f_\varepsilon & \text{on } \Gamma_D\ , \\ \sigma(\widetilde{u}_\varepsilon)n &=& g_\varepsilon & \text{on } \Gamma_N\ , \\ [\![\widetilde{u}_\varepsilon]\!] &=& 0 & \text{on } \partial B_\varepsilon\ , \\ [\![\sigma_\varepsilon(\widetilde{u}_\varepsilon)]\!]n &=& h_\varepsilon & \end{array}\right. \tag{5.60}$$

where $f_\varepsilon = -w_{\varepsilon|\Gamma_D}$, $g_\varepsilon = -\sigma(w_\varepsilon)n_{|\Gamma_N}$, and $h_\varepsilon = \widetilde{\sigma}n$, with the second order tensor field $\widetilde{\sigma}(x) = -(1-\gamma)[\sigma(u(x)) - \sigma(u(\widehat{x}))]$. From the above boundary value problem, it is possible to prove that the remainder $\widetilde{u}_\varepsilon$ enjoys an estimate of the form $\widetilde{u}_\varepsilon \approx O(\varepsilon^2)$ in an appropriated norm. In fact, before continuing, let us state the following important result:

Lemma 5.2 *Let $\widetilde{u}_\varepsilon$ be the solution of (5.60) or equivalently solution of the following variational problem:*

$$\widetilde{u}_\varepsilon \in \mathscr{U}_\varepsilon : \int_{\mathscr{D}} \sigma_\varepsilon(\widetilde{u}_\varepsilon)\cdot(\nabla\eta)^s = \int_{\Gamma_N} g_\varepsilon\cdot\eta + \int_{\partial B_\varepsilon} h_\varepsilon\cdot\eta \quad \forall\eta\in\mathscr{V}_\varepsilon\ , \tag{5.61}$$

with $\sigma_\varepsilon(\widetilde{u}_\varepsilon) = \gamma_\varepsilon\mathbb{C}(\nabla\widetilde{u}_\varepsilon)^s$, where the set $\mathscr{U}_\varepsilon$ and the space $\mathscr{V}_\varepsilon$ are defined respectively as

$$\mathscr{U}_\varepsilon := \{\varphi\in H^1(\mathscr{D}) : \varphi_{|\Gamma_D} = f_\varepsilon\}\ ,$$
$$\mathscr{V}_\varepsilon := \{\varphi\in H^1(\mathscr{D}) : \varphi_{|\Gamma_D} = 0\}\ .$$

Then, we have that the following estimate for the remainder $\widetilde{u}_\varepsilon$ holds true:

$$\|\widetilde{u}_\varepsilon\|_{H^1(\mathscr{D})} \le C\varepsilon^2\ , \tag{5.62}$$

with constant C independent of the small parameter ε.

Proof From the definition of function $h_\varepsilon = \widetilde{\sigma}n$, with n used to denote the unit normal vector field on ∂B_ε pointing toward to the center of the inclusion, we have

$$\begin{aligned}\int_{\partial B_\varepsilon} h_\varepsilon\cdot\eta &= \int_{\partial B_\varepsilon}\widetilde{\sigma}n\cdot\eta = -\int_{B_\varepsilon}\operatorname{div}(\widetilde{\sigma}\eta) = -\int_{B_\varepsilon}\operatorname{div}(\widetilde{\sigma})\cdot\eta - \int_{B_\varepsilon}\widetilde{\sigma}\cdot(\nabla\eta)^s \\ &= (1-\gamma)\int_{B_\varepsilon}\operatorname{div}(\sigma(u))\cdot\eta + (1-\gamma)\int_{B_\varepsilon}[\sigma(u)-\sigma(u(\widehat{x}))]\cdot(\nabla\eta)^s,\end{aligned} \tag{5.63}$$

where we have taken into account that $\widetilde{\sigma}(x) = -(1-\gamma)[\sigma(u(x)) - \sigma(u(\widehat{x}))]$. From this last result, the variational form (5.64) can be rewritten as follows:

$$\widetilde{u}_\varepsilon \in \mathscr{U}_\varepsilon : \int_{\mathscr{D}} \sigma_\varepsilon(\widetilde{u}_\varepsilon) \cdot (\nabla\eta)^s = \int_{\Gamma_N} g_\varepsilon \cdot \eta - \int_{B_\varepsilon} \widetilde{\sigma} \cdot (\nabla\eta)^s \quad \forall \eta \in \mathscr{V}_\varepsilon \,, \tag{5.64}$$

since $\operatorname{div}(\sigma(u)) = 0$. By taking $\eta = \widetilde{u}_\varepsilon - \varphi_\varepsilon$ as test function in (5.64), where $\varphi_\varepsilon \in \mathscr{U}_\varepsilon$ is the lifting of the Dirichlet boundary data f_ε on Γ_D, we have

$$\int_{\mathscr{D}} \sigma_\varepsilon(\widetilde{u}_\varepsilon) \cdot (\nabla\widetilde{u}_\varepsilon)^s = \int_{\Gamma_D} f_\varepsilon \cdot \sigma(\widetilde{u}_\varepsilon)n + \int_{\Gamma_N} g_\varepsilon \cdot \widetilde{u}_\varepsilon - \int_{B_\varepsilon} \widetilde{\sigma} \cdot (\nabla\widetilde{u}_\varepsilon)^s \,. \tag{5.65}$$

From the *Cauchy–Schwarz inequality* and the *trace theorem* there are

$$\begin{aligned} \left| \int_{\Gamma_D} f_\varepsilon \cdot \sigma(\widetilde{u}_\varepsilon)n \right| &\le \|f_\varepsilon\|_{H^{1/2}(\Gamma_D)} \|\sigma(\widetilde{u}_\varepsilon)n\|_{H^{-1/2}(\Gamma_D)} \\ &\le C_1\varepsilon^2 \|\nabla\widetilde{u}_\varepsilon\|_{L^2(\mathscr{D})} \le C_2\varepsilon^2 \|\widetilde{u}_\varepsilon\|_{H^1(\mathscr{D})} \,, \end{aligned} \tag{5.66}$$

and

$$\left| \int_{\Gamma_N} g_\varepsilon \cdot \widetilde{u}_\varepsilon \right| \le \|g_\varepsilon\|_{H^{-1/2}(\Gamma_N)} \|\widetilde{u}_\varepsilon\|_{H^{1/2}(\Gamma_N)} \le C_3\varepsilon^2 \|\widetilde{u}_\varepsilon\|_{H^1(\mathscr{D})} \,, \tag{5.67}$$

where we have used the fact that f_ε and g_ε have order $O(\varepsilon^2)$ on the exterior boundary $\partial\mathscr{D}$. By taking into account the definition $\widetilde{\sigma}(x) = -(1-\gamma)[\sigma(u(x)) - \sigma(u(\widehat{x}))]$, there is

$$\begin{aligned} \left| \int_{B_\varepsilon} \widetilde{\sigma} \cdot (\nabla\widetilde{u}_\varepsilon)^s \right| &\le \|\widetilde{\sigma}\|_{L^2(B_\varepsilon)} \|\nabla\widetilde{u}_\varepsilon\|_{L^2(B_\varepsilon)} \\ &\le C_4 \|\sigma(u) - \sigma(u(\widehat{x}))\|_{L^2(B_\varepsilon)} \|\nabla\widetilde{u}_\varepsilon\|_{L^2(B_\varepsilon)} \\ &\le C_5 \|x - \widehat{x}\|_{L^2(B_\varepsilon)} \|\nabla\widetilde{u}_\varepsilon\|_{L^2(B_\varepsilon)} \le C_6\varepsilon^2 \|\widetilde{u}_\varepsilon\|_{H^1(\mathscr{D})} \,, \end{aligned} \tag{5.68}$$

where we have used again the Cauchy–Schwarz inequality together with the interior elliptic regularity of function u. From these results, we obtain

$$\int_{\mathscr{D}} \sigma_\varepsilon(\widetilde{u}_\varepsilon) \cdot (\nabla\widetilde{u}_\varepsilon)^s \le C_7\varepsilon^2 \|\widetilde{u}_\varepsilon\|_{H^1(\mathscr{D})} \,. \tag{5.69}$$

Finally, from the *coercivity* of the bilinear form on the left-hand side of the above inequality, namely

$$c\|\widetilde{u}_\varepsilon\|^2_{H^1(\mathscr{D})} \le \int_{\mathscr{D}} \sigma_\varepsilon(\widetilde{u}_\varepsilon) \cdot (\nabla\widetilde{u}_\varepsilon)^s \,, \tag{5.70}$$

we obtain the result with $C = C_7/c$. □

5.1.4 Topological Derivative Evaluation

From the above elements, the integral (5.40) can be evaluated explicitly, which allows for collecting the terms in power of ε. Thus, it is possible to identify the function $f(\varepsilon)$ in (1.2) and compute the limit passage $\varepsilon \to 0$, leading to the final formula for the associated topological derivative. In particular, the integral (5.40) can be rewritten as

$$\mathscr{I}(\varepsilon) = -\frac{1-\gamma}{\gamma} \int_{B_\varepsilon} \sigma_\varepsilon(u_\varepsilon - u) \cdot (\nabla v)^s \ , \tag{5.71}$$

where we have used the definition for the contrast given by (5.3). After replacing the expansion (5.42) into the above equation we obtain

$$\begin{aligned} \mathscr{I}(\varepsilon) &= -\frac{1-\gamma}{\gamma} \int_{B_\varepsilon} \sigma_\varepsilon(w_\varepsilon + \widetilde{u}_\varepsilon) \cdot (\nabla v)^s \\ &= -\frac{1-\gamma}{\gamma} \int_{B_\varepsilon} \sigma_\varepsilon(w_\varepsilon) \cdot (\nabla v)^s + \mathscr{E}_1(\varepsilon) \ . \end{aligned} \tag{5.72}$$

The remainder $\mathscr{E}_1(\varepsilon)$ is defined as

$$\mathscr{E}_1(\varepsilon) = -\frac{1-\gamma}{\gamma} \int_{B_\varepsilon} \sigma_\varepsilon(\widetilde{u}_\varepsilon) \cdot (\nabla v)^s \ . \tag{5.73}$$

The Cauchy–Schwarz inequality together with the interior elliptic regularity of function u yield

$$|\mathscr{E}_1(\varepsilon)| \leq C_1 \|\nabla v\|_{L^2(B_\varepsilon)} \|\sigma_\varepsilon(\widetilde{u}_\varepsilon)\|_{L^2(B_\varepsilon)} \leq C_2 \varepsilon \|\nabla \widetilde{u}_\varepsilon\|_{L^2(\Omega)} \ . \tag{5.74}$$

From Lemma 5.2, we have

$$|\mathscr{E}_1(\varepsilon)| \leq C_3 \varepsilon \|\widetilde{u}_\varepsilon\|_{H^1(\Omega)} \leq C_4 \varepsilon^3 = O(\varepsilon^3) \ . \tag{5.75}$$

Now, let us comeback to the *expansion* (5.39), which can be written as

$$\begin{aligned} \mathscr{J}_\varepsilon(u_\varepsilon) - \mathscr{J}(u) &= -(1-\gamma) \int_{B_\varepsilon} \sigma(u) \cdot (\nabla v)^s - \frac{1-\gamma}{\gamma} \int_{B_\varepsilon} \sigma_\varepsilon(w_\varepsilon) \cdot (\nabla v)^s + \mathscr{E}_1(\varepsilon) \\ &= -(1-\gamma) \int_{B_\varepsilon} (\mathbb{I} + \mathbb{T}) \sigma(u(\widehat{x})) \cdot (\nabla v(\widehat{x}))^s + \sum_{i=1}^{3} \mathscr{E}_i(\varepsilon) \\ &= \pi \varepsilon^2 \mathbb{P}_\gamma \sigma(u(\widehat{x})) \cdot (\nabla v(\widehat{x}))^s + \sum_{i=1}^{3} \mathscr{E}_i(\varepsilon) \ , \end{aligned} \tag{5.76}$$

with $\mathbb{P}_\gamma = -(1-\gamma)(\mathbb{I}+\mathbb{T})$, where we have used the explicit solution for $\sigma_\varepsilon(w_\varepsilon)_{|B_\varepsilon}$ given by (5.58). The remainders $\mathscr{E}_2(\varepsilon)$ and $\mathscr{E}_3(\varepsilon)$ are respectively defined as

$$\mathscr{E}_2(\varepsilon) = -(1-\gamma)\int_{B_\varepsilon} (\sigma(u)\cdot(\nabla v)^s - \sigma(u(\widehat{x}))\cdot(\nabla v(\widehat{x}))^s)\,, \tag{5.77}$$

$$\mathscr{E}_3(\varepsilon) = -\frac{1-\gamma}{\gamma}\int_{B_\varepsilon} \sigma_\varepsilon(w_\varepsilon)\cdot((\nabla v)^s - (\nabla v(\widehat{x}))^s)\,, \tag{5.78}$$

which can be trivially bounded as follows:

$$|\mathscr{E}_2(\varepsilon)| \le C_1\varepsilon^3 = O(\varepsilon^3)\,, \tag{5.79}$$

$$|\mathscr{E}_3(\varepsilon)| \le C_2\varepsilon^3 = O(\varepsilon^3)\,, \tag{5.80}$$

where we have used the interior elliptic regularity of function u and the explicit solution (5.58). According to the estimates (5.75) and (5.79), the remainders $\mathscr{E}_1(\varepsilon)$, $\mathscr{E}_2(\varepsilon)$, and $\mathscr{E}_3(\varepsilon)$ are of order $o(\varepsilon^2)$. Therefore, from the expansion (5.76) we promptly identify function $f(\varepsilon) = \pi\varepsilon^2$ and thus the final formula for the *topological derivative* as [9, 45]

$$\mathscr{T}(\widehat{x}) = \mathbb{P}_\gamma\sigma(u(\widehat{x}))\cdot(\nabla v(\widehat{x}))^s \quad \forall\,\widehat{x}\in\Omega\,, \tag{5.81}$$

where the *polarization tensor* $\mathbb{P}_\gamma$ is given by the following fourth order isotropic tensor:

$$\mathbb{P}_\gamma = -\frac{1-\gamma}{1+\gamma a_2}\left((1+a_2)\mathbb{I} + \frac{1}{2}(a_1-a_2)\frac{1-\gamma}{1+\gamma a_1}\mathrm{I}\otimes\mathrm{I}\right)\,, \tag{5.82}$$

with the parameters a_1 and a_2 given by (5.57).

Remark 5.5 Note that the polarization tensor defined through (5.82) is isotropic because we are dealing with circular inclusions. For the polarization tensor regarding arbitrary-shaped inclusions, the reader may refer to the book by Ammari and Kang [5], for instance.

Remark 5.6 Formally, we can evaluate the limits $\gamma \to 0$ and $\gamma \to \infty$ in (5.82). For $\gamma \to 0$, the inclusion becomes a void and the transmission condition on the interface of the inclusion degenerates itself to the homogeneous Neumann boundary condition on the boundary of the resulting hole $B_\varepsilon(\widehat{x})$. Thus, in this particular case the *polarization tensor* is given by

$$\begin{aligned}\mathbb{P}_0 &= -(1+a_2)\mathbb{I} - \frac{a_1-a_2}{2}\mathrm{I}\otimes\mathrm{I}\\ &= -\frac{2\mu+\lambda}{\mu+\lambda}\left(2\mathbb{I} - \frac{\mu-\lambda}{2\mu}\mathrm{I}\otimes\mathrm{I}\right)\,.\end{aligned} \tag{5.83}$$

In addition, for $\gamma \to \infty$, the elastic inclusion becomes a rigid one and the polarization tensor is given by

$$\begin{aligned}\mathbb{P}_\infty &= \frac{1+a_2}{a_2}\mathbb{I} - \frac{a_1-a_2}{2a_1a_2}\mathrm{I}\otimes\mathrm{I} \\ &= \frac{2\mu+\lambda}{3\mu+\lambda}\left(2\mathbb{I} + \frac{\mu-\lambda}{2(\mu+\lambda)}\mathrm{I}\otimes\mathrm{I}\right) .\end{aligned} \tag{5.84}$$

The rigorous mathematical justification for these limit cases can be found in [7], for instance.

5.2 Topology Design Algorithm

In this section a topology optimization algorithm based on the topological derivative combined with a level-set domain representation method is presented. It has been proposed by Amstutz and Andrä [11] and consists basically in achieving a local optimality condition for the minimization problem (5.2), given in terms of the topological derivative and a level-set function. In particular, the domain $\Omega \subset \mathscr{D}$ and the complement $\mathscr{D} \setminus \Omega$ are characterized by a *level-set function* Ψ:

$$\Omega = \{x \in \mathscr{D} : \Psi(x) < 0\} \quad \text{and} \quad \mathscr{D} \setminus \Omega = \{x \in \mathscr{D} : \Psi(x) > 0\}, \tag{5.85}$$

where Ψ vanishes on the interface between Ω and $\mathscr{D} \setminus \Omega$. A local sufficient *optimality condition* for Problem (5.2), under a class of domain perturbations given by ball-shaped inclusions denoted by $B_\varepsilon(x)$, can be stated as [10]

$$\mathscr{T}(x) > 0 \quad \forall x \in \mathscr{D}, \tag{5.86}$$

where $\mathscr{T}(x)$ is the topological derivative of the shape functional $J(\Omega)$ at $x \in \mathscr{D}$ and $B_\varepsilon(x)$ is a ball of radius ε centered at $x \in \mathscr{D}$, as shown in Fig. 5.4. Therefore, let us define the quantity

$$g(x) := \begin{cases} -\mathscr{T}(x) \text{ if } \Psi(x) < 0, \\ +\mathscr{T}(x) \text{ if } \Psi(x) > 0, \end{cases} \tag{5.87}$$

which allows rewriting the condition (5.86) in the following equivalent form:

$$\begin{cases} g(x) < 0 \text{ if } \Psi(x) < 0, \\ g(x) > 0 \text{ if } \Psi(x) > 0. \end{cases} \tag{5.88}$$

We observe that (5.88) is satisfied, where the quantity g coincides with the level-set function Ψ up to a strictly positive factor, namely $\exists\, \tau > 0 : g = \tau\Psi$, or equivalently

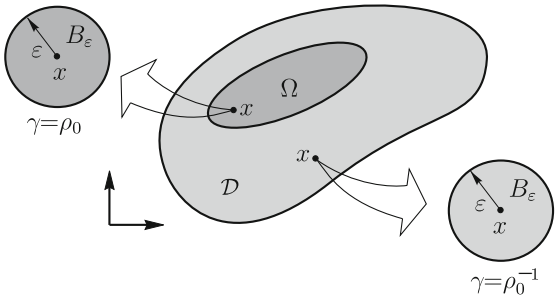

Fig. 5.4 Nucleation of a ball-shaped inclusion $B_\varepsilon(x)$

$$\theta := \arccos\left[\frac{\langle g, \Psi\rangle_{L^2(\mathscr{D})}}{\|g\|_{L^2(\mathscr{D})}\|\Psi\|_{L^2(\mathscr{D})}}\right] = 0, \tag{5.89}$$

which will be used as the optimality condition in the topology design algorithm, where θ is the angle in $L^2(\mathscr{D})$ between the functions g and Ψ.

Let us now explain the algorithm. We start by choosing an initial level-set function Ψ_0. In a generic iteration n, we compute the function g_n associated with the level-set function Ψ_n. Thus, the new level-set function Ψ_{n+1} is updated according to the following linear combination between the functions g_n and Ψ_n:

$$\begin{aligned} &\Psi_0 : \|\Psi_0\|_{L^2(\mathscr{D})} = 1, \\ &\Psi_{n+1} = \frac{1}{\sin\theta_n}\left[\sin((1-k)\theta_n)\Psi_n + \sin(k\theta_n)\frac{g_n}{\|g_n\|_{L^2(\mathscr{D})}}\right] \forall n \in \mathbb{N}, \end{aligned} \tag{5.90}$$

where θ_n is the angle between g_n and Ψ_n, and k is a step size determined by a line-search performed in order to decrease the value of the objective function $J(\Omega_n)$, with Ω_n used to denote the domain associated with Ψ_n. The process ends when the condition $\theta_n \leq \epsilon_\theta$ is satisfied at some iteration, where ϵ_θ is a given small numerical tolerance. Since we have chosen $\Psi_0 : \|\Psi_0\|_{L^2(\mathscr{D})} = 1$, by construction $\Psi_{n+1} : \|\Psi_{n+1}\|_{L^2(\mathscr{D})} = 1\ \forall n \in \mathbb{N}$. If at some iteration n the line-search step size k is found to be smaller, then a given numerical tolerance $\epsilon_k > 0$ and the optimality condition is not satisfied, namely $\theta_n > \epsilon_\theta$, then a mesh refinement of the hold-all domain $\mathscr{D}$ is carried out and the iterative process is continued. The resulting *topology design algorithm* is summarized in pseudo-code format in Algorithm 1. For further applications of this algorithm, see for instance [4, 14, 17, 49, 64, 85, 92].

In the context of topological-derivative-based topology optimization methods, the algorithms available in the literature usually combine topological derivatives with shape derivatives or level-set methods [1, 25, 36], leading to a two-stage shape/topology optimization procedure. More precisely, new holes are nucleated according to the topological derivative, while standard tools in shape optimization are used to move the new boundaries. In contrast, Algorithm 1 is based on the optimality condition (5.86) written in terms of the topological derivative and a level-set function, leading to a very simple and quite efficient one-stage algorithm driven

Algorithm 1: The topology design algorithm

input : $\mathscr{D}$, Ψ_0, ϵ_k, ϵ_θ;
output: the optimal topology $\Omega^\star$;

1 $n \leftarrow 0$;
2 $\Omega_n \leftarrow \Psi_n$;
3 compute the shape functional $J(\Omega_n)$;
4 compute the associated topological derivative $\mathscr{T}(x)$;
5 compute g_n and θ_n according to (5.87) and (5.89);
6 $\Psi_{\text{old}} \leftarrow \Psi_n$; $J_{\text{old}} \leftarrow J(\Omega_n)$; $J_{\text{new}} \leftarrow 1 + J_{\text{old}}$; $k \leftarrow 1$;
7 **while** $J_{\text{new}} > J_{\text{old}}$ **do**
8 compute Ψ_{new} according to (5.90);
9 $\Psi_n \leftarrow \Psi_{new}$;
10 execute lines 2 and 3;
11 $J_{\text{new}} \leftarrow J(\Omega_n)$;
12 $k \leftarrow k/2$;
13 **end while**
14 **if** $k < \epsilon_k$ **then**
15 try a mesh refinement;
16 $\Psi_{n+1} \leftarrow \Psi_n$; $n \leftarrow n + 1$;
17 **go to** line 2;
18 **else if** $\theta_n > \epsilon_\theta$ **then**
19 $\Psi_{n+1} \leftarrow \Psi_n$; $n \leftarrow n + 1$;
20 **go to** line 2;
21 **else**
22 **return** $\Omega^\star \leftarrow \Psi_n$;
23 **stop;**
24 **end if**

by the topological derivative only. However, how to efficiently use the topological derivative in the context of topology optimization deserves further investigation [19]. See Sect. 5.4 for an account of some open problems.

5.3 Numerical Results

The topological derivative has been specifically designed to deal with shape and topology optimization problems [1, 23, 25, 47, 57, 60, 73, 74, 76–78, 93]. In contrast to traditional topology optimization methods, the topological derivative formulation does not require a material model concept based on intermediary densities, so that interpolation schemes are unnecessary. These features are crucial in a wide range of applications, since the limitations arising from material model procedures are here naturally avoided. In addition, topological derivative has the advantage of providing an analytical form for the topological sensitivity which allows to obtain the optimal design in a few iterations or even in just one shot. Therefore, the resulting topology optimization algorithms are remarkably efficient and of simple computational implementation, since it features only a minimal number of user-defined algorithmic

parameters, as shown in Sect. 5.2, for instance. In this section, Algorithm 1 is applied in the context of compliance structural topology optimization and topology design of compliant mechanisms. In particular, the topology optimization problem we are dealing with consists in finding a subdomain $\Omega \subset \mathscr{D}$ that solves the following *minimization problem*:

$$\underset{\Omega \subset \mathscr{D}}{\text{Minimize}}\ \mathscr{F}_{\Omega}(u) = \mathscr{J}(u) + \beta|\Omega|\,, \tag{5.91}$$

where $\mathscr{J}(u)$ will be specified according to the application we are dealing with and $\beta > 0$ is a fixed multiplier used to impose a *volume constraint* in Ω of the form $|\Omega| \leq M$, with $M > 0$. In particular, by fixing different values of β we get different volume fractions at the end of the iterative process. For more sophisticated topological-derivative-based methods with volume constraint we refer the reader to [27], for instance. Since the last term in (5.91) represents the volume constraint, its associated topological derivative $\mathscr{T}_V(x)$ is trivially given by

$$\mathscr{T}_V(x) = \begin{cases} -1 \text{ if } x \in \Omega, \\ +1 \text{ if } x \in \mathscr{D} \setminus \Omega. \end{cases} \tag{5.92}$$

On the other hand, the first term in (5.91) depends on the state u solution of (5.6), so that the derivation of its topological derivative becomes much more involved, as presented in this chapter. Therefore, in this section we will adapt the obtained result (5.81) in such a way that it can be directly applied in the context of compliance structural topology optimization as well as in topology design of compliant mechanisms.

5.3.1 Structural Compliance Topology Optimization

Minimizing the structural flexibility under volume constraint is probably the most studied problem in the context of topology optimization. See the pioneering papers [20, 22] and also the book by Bendsøe [21], for instance. This classical problem is revisited here.

We start by setting $g = q$ in (5.14), which implies immediately that the adjoint state v, solution of (5.14), can be obtained as $v = -u$. See discussion in Remark 5.3. In this particular case, $\mathscr{J}(u)$ in (5.5) becomes the so-called compliance *shape functional*, namely

$$\mathscr{J}(u) = \int_{\Gamma_N} q \cdot u\,, \tag{5.93}$$

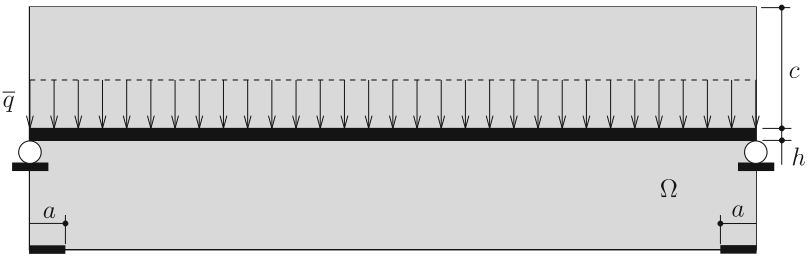

Fig. 5.5 Bridge design problem: initial guess and boundary conditions

where u is the solution of (5.6) and q is a given traction on Γ_N. By taking into account Remark 5.3 in result (5.81), the topological derivative of the compliance shape functional, denoted as $\mathscr{T}_C$, is given by

$$\mathscr{T}_C(x) = -\mathbb{P}_\gamma \sigma(u(x)) \cdot (\nabla u(x))^s \,, \tag{5.94}$$

where $\mathbb{P}_\gamma$ is the polarization tensor defined through (5.82). Finally, the topological derivative of the shape functional $\mathscr{F}_\Omega(u)$ in (5.91) is obtained from the sum

$$\mathscr{T}(x) = \mathscr{T}_C(x) + \beta \mathscr{T}_V(x) \quad \forall x \in \mathscr{D} \,, \tag{5.95}$$

where $\mathscr{T}_V(x)$ and $\mathscr{T}_C(x)$ are given by (5.92) and (5.94), respectively.

Let us now present a numerical example concerning the optimal *design of a bridge* structure borrowed from [75, Ch. 5, Sec. 5.2.5, p. 159]. The initial domain shown in Fig. 5.5 is represented by a rectangular panel of dimensions $180 \times 60\,\mathrm{m}^2$, which is clamped on the region $a = 9\,\mathrm{m}$ and submitted to a uniformly distributed traffic loading $q = 250 \times 10^3\,\mathrm{N/m}$. This load is applied on the dark strip of height $h = 3\,\mathrm{m}$, which is placed at a distance $c = 30\,\mathrm{m}$ from the top of the design domain. The dark strip will not be optimized. The Young modulus E and the Poisson ratio ν are set as $E = 210 \times 10^9\,\mathrm{N/m}^2$ and $\nu = 1/3$, respectively. The penalty parameter which appears in (5.91) is fixed to be $\beta = 10 \times 10^6$ and the contrast in (5.4) is set as $\rho_0 = 10^{-4}$. The topological derivative of the shape functional $\mathscr{F}_\Omega(u)$ obtained at the first iteration of the shape and topology optimization numerical procedure is shown in Fig. 5.6, where white to black levels mean smaller (negative) to higher (positive) values. This picture induces a level-set domain representation for the optimal shape, as proposed in [11]. See Algorithm 1. The resulting topology design obtained in the form of a well-known tied-arch bridge structure, which is acceptable from practical point of view, is shown in Fig. 5.7. Usually it is a local minimizer obtained numerically for the compliance minimization with volume constraint. Indeed, there is a lack of sufficient optimality conditions for such shape optimization problems [15]. The convergence curves for the angle θ_n and shape functional $J(\Omega_n)$ are shown in Fig. 5.8, where the picks come out from the mesh refinement procedure.

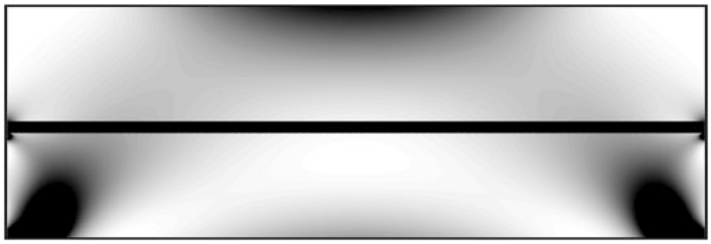

Fig. 5.6 Bridge design problem: topological derivative in the hold-all domain

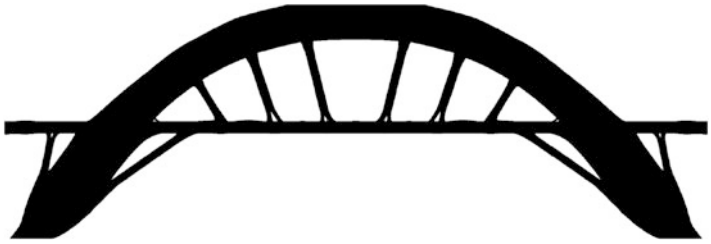

Fig. 5.7 Bridge design problem: optimal domain [75]

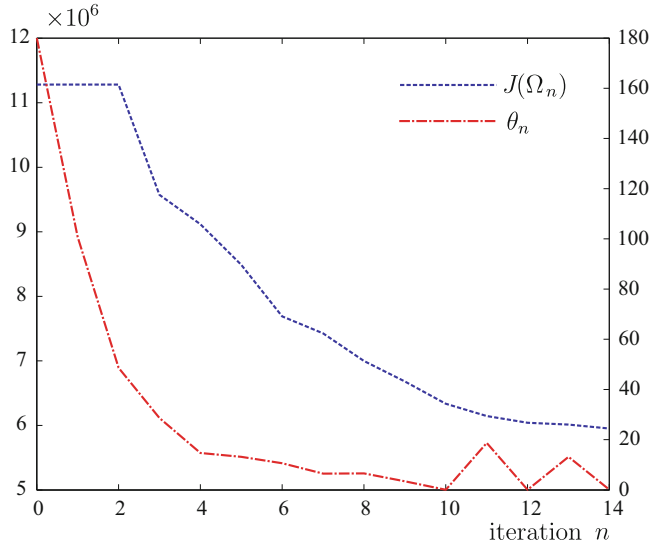

Fig. 5.8 Bridge design problem: convergence curves for the angle θ_n (dashed-dot red line) and shape functional $J(\Omega_n)$ (dashed blue line)

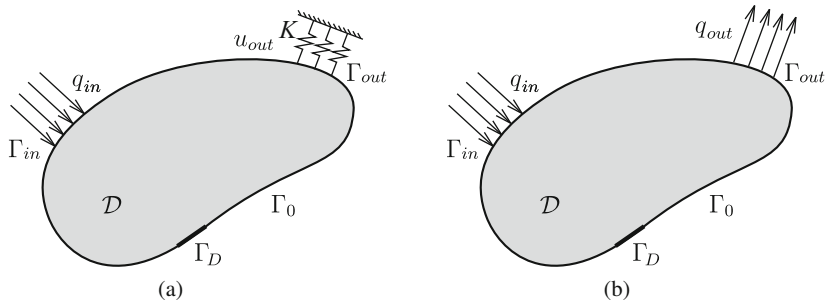

Fig. 5.9 Design of compliant mechanisms: problem setting. (**a**) Original model. (**b**) Surrogate model

5.3.2 *Topology Design of Compliant Mechanisms*

Compliant mechanisms are mechanical devices composed by one single peace that transforms simple inputs into complex movements by amplifying and changing their direction [2, 26, 29, 59, 63, 65, 69, 87]. Hence they are easy to fabricate and miniaturize and have no need for lubrication. Although these ideas are not new [26], compliant mechanisms have received considerable attention in recent years. This fact is due to manufacturing at a very small scale, the introduction of new advanced materials, and the fast development of Micro-Electro-Mechanical Systems [37]. Since such microtools are capable to perform precise movements, the spectrum of their applications has become broader including microsurgery, nanotechnology processing, cell manipulation, among others.

Therefore, let us adapt the problem stated in Sect. 5.1 to the context of topology design of compliant mechanisms. We start by splitting Γ_N into three mutually disjoint parts Γ_{in}, Γ_{out}, and Γ_0, such that $\Gamma_N = \Gamma_{\text{in}} \cup \Gamma_{\text{out}} \cup \Gamma_0$. The idea is to maximize the output displacement u_{out} on Γ_{out} in some direction for a given input excitation q_{in} on Γ_{in}. The exterior medium is represented by springs with stiffness K, attached to the output port Γ_{out}, as shown in Fig. 5.9a. The springs are then replaced by the expected boundary reaction q_{out} on Γ_{out}. In this way, the output displacement is going to be indirectly constrained by such given reaction. See sketch in Fig. 5.9b. From this discussion, we define $q = q_{\text{in}}$ on Γ_{in}, $q = q_{\text{out}}$ on Γ_{out}, and $q = 0$ on Γ_0. Thus, the variational problem (5.6) can be rewritten as

$$u \in \mathcal{V} : \int_{\Omega} \sigma(u) \cdot (\nabla \eta)^s = \int_{\Gamma_{\text{in}}} q_{\text{in}} \cdot \eta + \int_{\Gamma_{\text{out}}} q_{\text{out}} \cdot \eta \quad \forall \eta \in \mathcal{V} \,, \tag{5.96}$$

with $\sigma(u) = \rho \mathbb{C} (\nabla u)^s$. In addition, we set $g = q_{\text{in}}$ on Γ_{in}, $g = \kappa q_{\text{out}}$ on Γ_{out}, and $g = 0$ on Γ_0, so that the *shape function* (5.5) becomes

$$\mathcal{J}(u) = \int_{\Gamma_{\text{in}}} q_{\text{in}} \cdot u + \kappa \int_{\Gamma_{\text{out}}} q_{\text{out}} \cdot u \,. \tag{5.97}$$

Finally, the associated adjoint system (5.14) can be stated as

$$v \in \mathscr{V} : \int_{\Omega} \sigma(v) \cdot (\nabla \eta)^s = -\int_{\Gamma_{\text{in}}} q_{\text{in}} \cdot \eta - \kappa \int_{\Gamma_{\text{out}}} q_{\text{out}} \cdot \eta \in \mathscr{V} , \tag{5.98}$$

with $\sigma(v) = \rho \mathbb{C}(\nabla v)^s$, where $\kappa > 0$ is a weight parameter. For more details concerning the adopted formulation, the reader may refer to [63], for instance. In this particular case, the topological derivative of the shape functional $\mathscr{F}_{\Omega}(u)$ in (5.91) is given by the sum

$$\mathscr{T}(x) = \mathscr{T}_E(x) + \beta \mathscr{T}_V(x) \quad \forall x \in \Omega , \tag{5.99}$$

where the topological derivative of the volume constraint $\mathscr{T}_V(x)$ is given by (5.92) whereas the topological derivative of the mechanism effectiveness $\mathscr{T}_E(x)$ can be obtained from (5.81), namely

$$\mathscr{T}_E(x) = \mathbb{P}_{\gamma} \sigma(u(x)) \cdot (\nabla v(x))^s , \tag{5.100}$$

where u and v are the solutions of (5.96) and (5.98), respectively, and $\mathbb{P}_{\gamma}$ is the polarization tensor from (5.82).

In order to fix these ideas, let us present a numerical example where the minimization problem (5.91) is solved with the help of Algorithm 1. It consists in an inverter *mechanism design*. The hold-all domain representing the initial guess is given by a square clamped on the left corners, while the loads $q_{\text{in}} = (2, 0)$ and $q_{\text{out}} = (1, 0)$ are respectively applied on the middle of the left and right edges, respectively. See Fig. 5.10a. The penalty parameter in (5.91) is set as $\beta = 3$ and the weight parameter which appears in (5.97) is given by $\kappa = 10$. Finally, the Young modulus, the Poisson ratio, and the contrast in (5.4) are respectively given by $E = 1$, $\nu = 0.3$, and $\rho_0 = 10^{-4}$. The amplified deformations of the final obtained solution are presented in Fig. 5.10b, where we observe that the obtained mechanism performs the desired movement. The convergence curves for the angle θ_n and shape functional $J(\Omega_n)$ are shown in Fig. 5.11.

5.4 Final Remarks

In this chapter a topology optimization algorithm based on the topological derivative and the level-set domain representation method has been presented. In particular, Algorithm 1 has been proposed in [11] to achieve a local optimality condition for the minimization problem under consideration, which is given in terms of the topological derivative and an appropriated level-set function. This means that the topological derivative is in fact used within the numerical procedure as a steepest-descent direction similar to methods based on the gradient of the cost functional. The topological derivative represents the *exact* first order variation of the shape

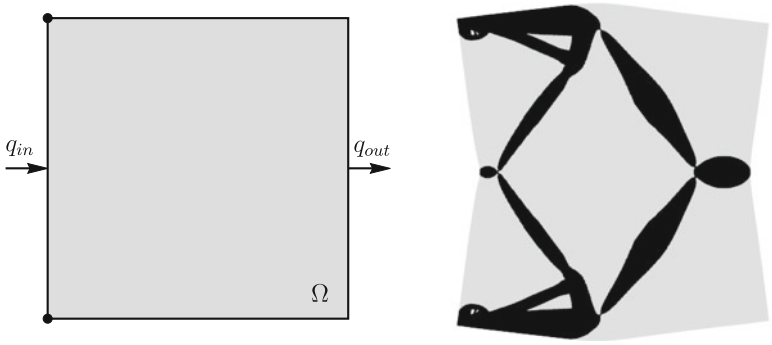

(a) initial guess (b) optimal domain

Fig. 5.10 Inverter design problem: initial guess and boundary conditions (**a**) and deformed configuration of the optimal domain (**b**)

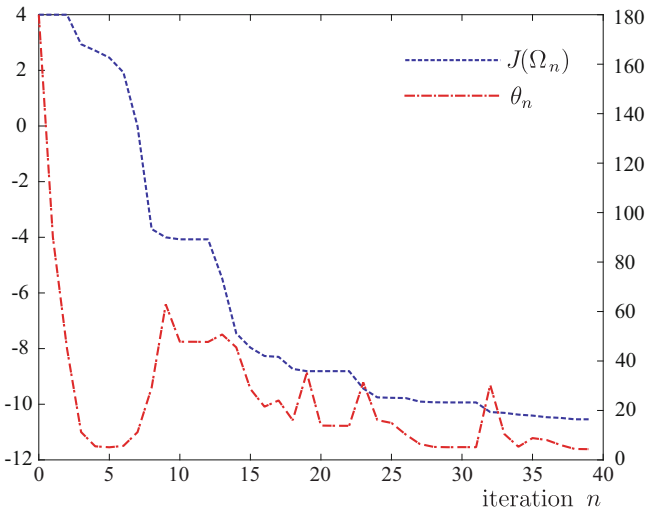

Fig. 5.11 Inverter design problem: convergence curves for the angle θ_n (dashed-dot red line) and shape functional $J(\Omega_n)$ (dashed blue line)

functional with respect to the nucleation of small singular domain perturbations, so that the resulting topology design algorithm converges in few iterations by using a minimal number of user defined algorithmic parameters, as shown in the numerics presented in Sect. 5.3. Furthermore, the topological derivative follows in fact the basic rules of Differential Calculus, which allows for applying it in the context of multi-objective topology optimization algorithms by using e.g., the known formulas already available in the literature. Finally, in contrast to traditional topology optimization methods, the topological derivative formulation does not require any material model concept based on intermediary densities, so that no

interpolation schemes are used within the numerical procedures. This feature is crucial in the topology design problem, since the difficulties arising from material model procedures are here naturally avoided. Therefore, the topological derivative method can be seen, when applicable, as a simple alternative method for numerical solution of a wide class of topology optimization problems. For future development of the topological-derivative-based method, we highlight the following:

According to Sect. 5.3, there are numerical evidences showing that Algorithm 1 converges in most cases. However, from the theoretical point of view, only partial results can be found in the literature. See for instance [10], where the convergence of Algorithm 1 has been analyzed in the particular case of an optimal control problem with respect to characteristic functions of small sets. Therefore, the most important theoretical problem to be solved concerns the convergence of Algorithm 1 in general.

The topological derivative concept has also been shown to be effective in solving a certain class of inverse problems [13, 30, 40, 44, 52, 55, 82, 86, 91]. In particular, stability and resolution analysis for a topological-derivative-based imaging functional have been presented in the context of the Helmholtz equation [6]. However, such analysis is missing for other classes of inverse problems, including gravimetry and EIT, for instance. In this direction, a new branch of research arises, which consists in solving a wide range of reconstruction problems with the help of second order topological derivatives [28, 41–43, 53, 66, 84]. In this context, many interesting questions arise, including on how to efficiently use higher order expansions, for instance.

Synthesis and optimal design of materials in a multiscale framework have been considered in [46] and further developed in [16], where the topological derivative of the homogenized elasticity tensor has been obtained. Extension to the dynamic case is a difficult and interesting research topic, where inertial forces acting at the microscale may produce unexpected macroscopic constitutive behavior. Finally, a new emerging research field consists in the design of new materials by considering the strain gradient homogenized constitutive tensor. From the theoretical point of view, a deep question arises in the context of topological derivatives associated with asymptotic models in general, including multiscale and dimension reduction, for instance. In particular, both objects come out from a limit passage procedure, one representing the size of the topological perturbation and the other one controlling the scale. It is not clear whether these limits commute or not. Actually, different results are expected after interchanging the order of these limits.

Topology design of structures taking into account more realistic scenario such as anisotropic elasticity [24, 48], transient wave equations [32], and evolution variational inequalities is a difficult and challenging problem, which requires further development from both theoretical and numerical points of views.

Topological-derivative-based topology design in multiphysics taking into account multiobjective shape functionals is an important and difficult subject of research, which also deserves investigation. Design of antenna and wave guides in nanophotonics is an example of modern application. It can be handled with the use of the domain decomposition technique presented in Chap. 4, for instance.

The Griffith-Francfort-Marigo damage model adopted in [3] and later in [95] and [97] does not distinguish between traction and compression stress states in the damage evolution process. Hence, it is unsuitable for describing the crack closure phenomenon. Therefore, the development of the topological derivative theory for functionals which consider distinct criteria in traction and in compression deserves investigation. However, it is well known that such modeling leads to a class of nonlinear elasticity systems, so that these extensions are expected to be difficult. See also closely related works dealing with crack nucleation sensitivity analysis [8, 94] and crack propagation control [96].

Extension to nonlinear problems in general can be considered as the main challenge in the theoretical development of the topological derivative method. The difficulty arises when the nonlinearity comes out from the main part of the operator, which at the same time suffers a topological perturbation. It is the case of nucleation of holes in plasticity and finite deformations in solid mechanics or small obstacles in compressive fluid flow, for instance. See the recent publication [12] dealing with topological derivatives for a class of quasilinear elliptic equations.

5.5 Exercises

1. By taking $\rho = 1$ in (5.12), derive the Navier system (5.13).
2. From the weak formulation (5.19), derive the strong form (5.20) and discuss the transmission condition on the interface ∂B_ε.
3. By using separation of variable technique, find the stress distribution around the inclusion B_ε, which is the solution of the exterior boundary value problem (5.47). **Hint:** Consult the book by Little [62] and look for the Airy functions in polar coordinate system.
4. Take into account Remark 5.4 and derive the closed formula for the isotropic and uniform fourth order tensor $\mathbb{T}$ given by (5.59) in the form $\mathbb{T} = \alpha_1 \mathbb{I} + \alpha_2 \mathrm{I} \otimes \mathrm{I}$, by finding the coefficients α_1 and α_2 explicitly.
5. Repeat the derivations presented in Remark 3.1 to find a general representation for the polarization tensor in elasticity.

   Hint: After introducing the notation $w(\varepsilon^{-1}x) := \varepsilon^{-1} w_\varepsilon(x)$ and the change of variable $\xi = \varepsilon^{-1}x$, write $w(\xi)$ as a linear combination of the components of $\sigma(u(\widehat{x}))$ as follows $w(\xi) = \sigma(u(\widehat{x}))_{ij}\, v^{(ij)}(\xi)$. Then replace it into the exterior problem (5.47) to obtain a set of canonical variational problems of the form:

$$v^{(ij)} \in \mathscr{W} \,:\, \int_{\mathbb{R}^2} \gamma_\omega \sigma_\xi(v^{(ij)}) \cdot (\nabla_\xi \eta)^s = (1-\gamma)(e_i \otimes e_j) \cdot \int_\omega (\nabla_\xi \eta)^s \quad \forall \eta \in \mathscr{W}, \tag{5.101}$$

   where $\sigma_\xi(v^{(ij)}) = \mathbb{C}(\nabla_\xi v^{(ij)})^s$. The quotient space $\mathscr{W}$ is defined as $\mathscr{W} := \{\varphi \in H^1(\mathbb{R}^2)/\mathbb{R}\}$ and the contrast γ_ω is given by $\gamma_\omega = 1$ in $\mathbb{R}^2 \setminus \omega$ and $\gamma_\omega = \gamma$ in ω. Finally, comeback to (5.76) and write the polarization tensor as follows:

$$\mathbb{P}_\gamma = -(1-\gamma)\left(\mathbb{I} + \frac{1}{|\omega|}\int_\omega \sigma_\xi(v^{(kl)})_{ij}(e_i \otimes e_j \otimes e_k \otimes e_l)\right) . \tag{5.102}$$

6. Code Algorithm 1 and reproduce the numerical examples presented in Sect. 5.3.
7. Study and discuss the list of open problems presented at the end of Sect. 5.4.